

Differential Space-Code Modulation for Interference Suppression

Jianhua Liu, *Student Member, IEEE*, Jian Li, *Senior Member, IEEE*, Hongbin Li, *Member, IEEE*, and Erik G. Larsson, *Student Member, IEEE*

Abstract—Space-time coding has been receiving much attention recently due to its potentials offered by fully exploiting the spatial and temporal diversities of multiple transmit and receive antennas. A differential space-time modulation (DSTM) scheme was recently proposed for demodulation without channel state information, which is attractive in fast fading channels where accurate channel estimates are difficult to obtain. However, this technique is sensitive to interference and is likely to deteriorate or even break down in a wireless environment, where interference (including intentional and unintentional jamming) signals exist. We propose a new coding and modulation scheme, referred to as the *differential space-code modulation* (DSCM), which is interference resistant. Our focus is on single-user communications. We show that DSCM outperforms DSTM significantly when interference is present. This advantage is achieved at the cost of a lower data rate or a wider bandwidth or a combination of both. To alleviate this problem, a high-rate DSCM (HR-DSCM) scheme is also presented, which increases the data rate considerably at the cost of a slightly higher bit-error rate (BER), while still maintaining the interference suppression capability.

Index Terms—Interference suppression, smart antennas, space-time coding, spread spectrum, wireless communications.

I. INTRODUCTION

THE CAPACITY of a wireless communication system can be increased drastically by employing multiple transmit/receive antennas [1], [2]. Traditionally, spatial diversity was mainly exploited by receivers. In fact, receiver antenna diversity is being used by base stations to improve the reception in current cellular systems. Yet, transmit diversity is just beginning to attract more attention [3].

Recently, Alamouti [4] proposed a simple yet useful transmit diversity scheme, which fully exploits the spatial diversity offered by multiple transmit antennas and improves the overall performance of wireless communication systems. This scheme is one of many interesting techniques emerging in the field of space-time coding (see, e.g., [3] and the references therein). However, Alamouti's method, as well as many other transmit diversity schemes, such as those in [5]–[7], are based on the assumption that perfect channel state information (CSI) is

available at the receiver or at least that it can be accurately estimated by, for example, transmitting training symbols. Although training is a feasible approach to obtain the CSI when the channel is stationary or changes slowly, it will incur excessive overhead or even break down when the channel experiences fast fading.

More recently, differential space-time modulation (DSTM) schemes were introduced as extensions of the traditional differential phase shift keying (DPSK) scheme [8]–[11]. DSTM schemes obviate the need for channel estimation at the receiver while maintaining the desired properties of space-time coding techniques. Yet, these schemes are sensitive to interference due to the assumption of spatially and temporally white Gaussian noise in the receive antenna array outputs. Their performance degrades significantly in the presence of even relatively mild interference and breaks down completely when strong interference exists.

In this paper, we present a new spatial/temporal coding and modulation scheme referred to as the *differential space-code modulation* (DSCM), whereby *code* refers to the spreading code used in this modulation scheme. The DSCM scheme exploits the merits offered by multiple transmit and multiple receive antennas as well as the spread spectrum technology for interference suppression. By making use of the unitary group codes [11]–[14], the proposed scheme entails a simple receiver structure. By choosing appropriate spreading sequences for DSCM, we can capture the statistics of the additive channel noise and interference. This statistic is then used for interference suppression by taking advantage of the degree-of-freedom offered by the multiple receive antennas. Our focus is on single-user communications. We demonstrate with simulation examples that DSCM significantly outperforms DSTM when interference (including intentional and unintentional jamming) signals, especially strong ones, exist. This advantage is achieved at the cost of a lower data rate or a wider bandwidth or a combination of both. To alleviate this problem, we also propose a *high-rate* DSCM (HR-DSCM) scheme, which is an extension of DSCM when used with orthogonal spreading sequences. HR-DSCM increases the data rate considerably at the cost of a slightly higher bit-error rate (BER) while still maintaining the interference suppression capability.

The remainder of the paper is organized as follows. Section II briefly reviews the unitary group code based DSTM scheme. Section III presents the new DSCM scheme. Extension of the DSCM scheme to the HR-DSCM scheme is discussed in Section IV. Simulation results are presented in Section V. Finally, we deliver our comments and conclusions in Section VI.

Manuscript received August 15, 2000; revised April 30, 2001. This work was supported in part by the National Science Foundation under Grant CCR-0097114 and the Swedish Foundation for Strategic Research (SSF). The associate editor coordinating the review of this paper and approving it for publication was Dr. Nicholas D. Sidiropoulos.

J. Liu, J. Li, and E. G. Larsson are with the Department of Electrical and Computer Engineering, University of Florida, Gainesville, FL 32611 USA (e-mail: li@dsp.ufl.edu).

H. Li is with the Department of Electrical and Computer Engineering, Stevens Institute of Technology, Hoboken, NJ 07030-5991 USA.

Publisher Item Identifier S 1053-587X(01)05853-6.

II. REVIEW OF DSTM

To facilitate our presentation, we first briefly review the unitary group code based differential space-time modulation of [8]–[11]. Let

- M number of transmit antennas;
- N number of receive antennas;
- L time length of a space-time code.

Let \mathbf{C}_k be the k th $M \times L$ space-time code to be transmitted by the M antennas over L time samples. For differential space-time coding, \mathbf{C}_k satisfies [11]

$$\mathbf{C}_k \mathbf{C}_k^H = L \mathbf{I}_M \quad (1)$$

where $(\cdot)^H$ denotes the conjugate transpose, \mathbf{I}_M is an $M \times M$ identity matrix, and

$$\mathbf{C}_k = \mathbf{C}_{k-1} \mathbf{G}_k, \quad \mathbf{C}_0 = \mathbf{D} \quad (2)$$

where \mathbf{D} is a fixed and known matrix, and \mathbf{G}_k is the k th information matrix, which is an element of a group of unitary matrices. For example, for $M = L = 2$, the pair

$$\mathcal{G} = \left\{ \pm \begin{bmatrix} 1 & 0 \\ 0 & 1 \end{bmatrix}, \pm \begin{bmatrix} 0 & 1 \\ -1 & 0 \end{bmatrix} \right\}, \quad \mathbf{D} = \begin{bmatrix} 1 & -1 \\ 1 & 1 \end{bmatrix} \quad (3)$$

is a unitary group code over the BPSK constellation $\{1, -1\}$ and $\mathbf{G}_k \in \mathcal{G}$. Each information bit pair in $\{00, 01, 10, 11\}$ corresponds to an element in \mathcal{G} .

Let $\mathbf{H} \in \mathcal{C}^{N \times M}$ be the unknown fading matrix in a flat fading environment, and let $\mathbf{E}_k \in \mathcal{C}^{N \times L}$ be the additive noise matrix. The array received data matrix $\mathbf{Y}_k \in \mathcal{C}^{N \times L}$ has the form [11]

$$\mathbf{Y}_k = \sqrt{\rho_M} \mathbf{H} \mathbf{C}_k + \mathbf{E}_k \quad (4)$$

where $\rho_M = \rho/M$ with ρ denoting the signal-to-noise ratio (SNR) per receive antenna. Each of the elements of \mathbf{H} and \mathbf{E}_k is assumed to be independently and identically distributed complex Gaussian random variable with zero-mean and *unit* variance, i.e.,

$$\text{vec}(\mathbf{H}) \sim \mathcal{N}(\mathbf{0}, \mathbf{I}_{MN}), \quad \text{vec}(\mathbf{E}_k) \sim \mathcal{N}(\mathbf{0}, \mathbf{I}_{NL}) \quad (5)$$

where $\text{vec}(\cdot)$ denotes the column vector obtained by stacking the columns of a matrix on top of each other. Then, a simple differential receiver has the form [11]

$$\hat{\mathbf{G}}_k = \arg \max_{\mathbf{G}_k \in \mathcal{G}} \text{Re} \left\{ \text{tr} (\mathbf{Y}_k^H \mathbf{Y}_{k-1} \mathbf{G}_k) \right\} \quad (6)$$

where $\text{Re}\{\cdot\}$ denotes the real part of the argument, and $\text{tr}(\cdot)$ denotes the trace of a matrix.

Since the additive noise is assumed to be spatially and temporally white, the performance of this receiver is bound to degrade until complete failure in the presence of interference. In the following, we introduce a new coding/modulation scheme that facilitates a novel design of receivers that are interference resistant.

III. DIFFERENTIAL SPACE-CODE MODULATION

We propose to integrate the strengths of the unitary group code based DSTM with the spread spectrum technology

to achieve interference suppression by fully exploiting the degree of freedom offered by the multiple receive antennas. Throughout our discussions, we will consider the case of a single user in the presence of unknown and arbitrary interference signals over which we have no control.

The idea of the unitary group code based *differential space-code modulation* we propose herein to transmit simultaneously two space-time codes over J chips for the k th information matrix \mathbf{G}_k , where J is the length of the known spreading sequences. The different columns of the two space-time codes $\mathbf{C}_{k,0}$ and $\mathbf{C}_{k,1}$ are modulated with different spreading sequences (orthogonal or close to orthogonal). These spreading sequences are transmitted *at the same time* and are used to separate the signals corresponding to the different columns of the space-time codes. In this DSCM scheme, \mathbf{G}_k is related to $\mathbf{C}_{k,0}$ and $\mathbf{C}_{k,1}$ as follows:

$$\mathbf{C}_{k,1} = \mathbf{C}_{k,0} \mathbf{G}_k \quad (7)$$

where either $\mathbf{C}_{k,0} = \mathbf{D}$ [such as the \mathbf{D} in (3)] or $\mathbf{C}_{k,0} = \mathbf{C}_{k-1,1}$. Note that DSCM is based on the intracodeword differential structure rather than the conventional time-domain differential structure.

At the j th chip for the k th information matrix \mathbf{G}_k , the receiver array output $\mathbf{x}_k(j) \in \mathcal{C}^{N \times 1}$ has the form

$$\mathbf{x}_k(j) = \sqrt{\rho_M} \mathbf{H}_k [\mathbf{C}_{k,0} \quad \mathbf{C}_{k,1}] \mathbf{d}(j) + \mathbf{e}_k(j) \quad (8)$$

$$j = 1, \dots, J$$

where $\mathbf{H}_k \in \mathcal{C}^{N \times M}$ is the unknown fading matrix for time interval k , $\{\mathbf{d}(j) \in \mathcal{R}^{2L \times 1}, j = 1, 2, \dots, J\}$ denote the $2L$ known spreading sequences of length J , and the interference and noise vector $\mathbf{e}_k(j) \sim \mathcal{N}(\mathbf{0}, \mathbf{Q}_k)$. Here, \mathbf{Q}_k denotes the arbitrary unknown covariance matrix of the interference and noise. For notational simplicity, let

$$\mathbf{A}_k \triangleq \sqrt{\rho_M} \mathbf{H}_k [\mathbf{C}_{k,0} \quad \mathbf{C}_{k,1}]. \quad (9)$$

Then, (8) becomes

$$\mathbf{x}_k(j) = \mathbf{A}_k \mathbf{d}(j) + \mathbf{e}_k(j), \quad j = 1, \dots, J. \quad (10)$$

With the extra flexibility offered by the space-code modulation, we can choose the spreading sequences to our advantage. In particular, we will use the spreading sequences to capture the statistics of the interference and noise vector $\mathbf{e}_k(j)$ and to obtain an initial estimate of \mathbf{A}_k . Once we have this information, we can devise a receiver that achieves interference suppression and yet is remarkably similar in structure to the one in (6).

The DSCM scheme can be used with either orthogonal or nonorthogonal spreading codes. However, as shown in Appendix A, using the DSCM scheme with orthogonal spreading codes leads to a significantly simplified receiver. Receiver design based on the DSCM scheme is discussed in detail in Appendix A. Here, we summarize the DSCM receiver when unit-energy orthogonal spreading codes (e.g., the Hadamard codes) are employed as follows.

- 1) Calculate the covariance matrices:

$$\hat{\mathbf{R}}_{dx_k} = \frac{1}{J} \sum_{j=1}^J \mathbf{d}(j) \mathbf{x}_k^H(j) \quad (11)$$

and

$$\hat{\mathbf{R}}_{x_k x_k} = \frac{1}{J} \sum_{j=1}^J \mathbf{x}_k(j) \mathbf{x}_k^H(j). \quad (12)$$

- 2) Compute the estimates of \mathbf{A}_k , \mathbf{Q}_k and $\tilde{\mathbf{Q}}_k$:

$$\hat{\mathbf{A}}_k = J \hat{\mathbf{R}}_{dx_k}^H \quad (13)$$

$$\hat{\mathbf{Q}}_k = \hat{\mathbf{R}}_{x_k x_k} - J \hat{\mathbf{R}}_{dx_k}^H \hat{\mathbf{R}}_{dx_k} \quad (14)$$

and

$$\tilde{\mathbf{Q}}_k = \hat{\mathbf{Q}}_k^{-1/2} \left(\mathbf{I} + \frac{1}{MN} \text{tr} \left[\hat{\mathbf{A}}_k \hat{\mathbf{A}}_k^H \right] \hat{\mathbf{Q}}_k^{-1} \right)^{-1} \hat{\mathbf{Q}}_k^{-1/2}. \quad (15)$$

- 3) Perform ‘‘pre-whitening’’:

$$\tilde{\mathbf{A}}_k = \hat{\mathbf{Q}}_k^{-1/2} \hat{\mathbf{A}}_k \triangleq \begin{bmatrix} \tilde{\mathbf{B}}_{k,0} & \tilde{\mathbf{B}}_{k,1} \end{bmatrix}. \quad (16)$$

- 4) Determine the estimate of \mathbf{G}_k :

$$\hat{\mathbf{G}}_k = \arg \max_{\mathbf{G}_k \in \mathcal{G}} \text{Re tr} \left\{ \mathbf{G}_k \tilde{\mathbf{B}}_{k,1}^H \tilde{\mathbf{Q}}_k \tilde{\mathbf{B}}_{k,0} \right\}. \quad (17)$$

We remark that we should choose J to be larger than the number of receive antennas so that the statistics of the interference can be reliably estimated. Yet J must be small enough to adapt quickly to the changing channel and interference environment. Note that the Hadamard codes employed in the DSCM scheme have unit energy. As such, the power level of the DSCM scheme is $2L/J$ times of that of the DSTM scheme, given the same value of ρ_M and the same channel. For large J , $2L/J \ll 1$. Hence, the DSCM scheme is more suitable for covert communications than the DSTM scheme. Note, however, that these advantages of the DSCM scheme are achieved at the cost of a lower data rate or a wider bandwidth or a combination of both due to the use of the spreading sequences.

IV. HIGH-RATE DSCM

To improve the data rate of DSCM, we can employ group codes of larger cardinality [12]. An alternative way, which we advocate in this paper, is to transmit several space-time code matrices simultaneously. This leads to a modulation scheme that we will refer to as the *high-rate differential space-code modulation* (HR-DSCM). In particular, $P-1$ information matrices $\mathbf{G}_{k,1}, \mathbf{G}_{k,2}, \dots, \mathbf{G}_{k,P-1}$ are transmitted simultaneously as the k th block of P unitary group codes. These matrices are differentially coded according to

$$\mathbf{C}_{k,0} = \mathbf{D} \quad \text{or} \quad \mathbf{C}_{k-1,P-1} \quad (18)$$

$$\mathbf{C}_{k,1} = \mathbf{C}_{k,0} \mathbf{G}_{k,1} \quad (19)$$

\vdots

$$\mathbf{C}_{k,P-1} = \mathbf{C}_{k,P-2} \mathbf{G}_{k,P-1}. \quad (20)$$

The receiver output $\mathbf{x}_k(j) \in \mathcal{C}^{N \times 1}$ still has the form

$$\mathbf{x}_k(j) = \mathbf{A}_k \mathbf{d}(j) + \mathbf{e}_k(j), \quad j = 1, \dots, J. \quad (21)$$

However, \mathbf{A}_k is now given by

$$\mathbf{A}_k = \sqrt{\rho_M} \mathbf{H}_k [\mathbf{C}_{k,0} \quad \mathbf{C}_{k,1} \quad \dots \quad \mathbf{C}_{k,P-1}] \in \mathcal{C}^{N \times PL} \quad (22)$$

and, likewise, the dimension of $\mathbf{d}(j)$ is now $PL \times 1$. Note that the signal power of the HR-DSCM scheme, when used with unit-energy orthogonal spreading codes and given the same ρ_M and channel condition, is PL/J times that of DSTM. Hence, HR-DSCM is less covert than DSCM (which has $P = 2$) when $P > 2$. The bit rate (in bits/s/Hz) of HR-DSCM is $R(P-1)L/J$, where R is the bit rate of DSTM and is equal to $\log_2 |\mathcal{G}|/L$, with $|\mathcal{G}|$ denoting the number of unitary matrices in \mathcal{G} .

Similar to the DSCM receiver, using orthogonal spreading codes significantly simplifies the complexity of the HR-DSCM receiver. In particular, due to the orthogonality of the spreading codes, we can decouple the detection of the $P-1$ information matrices $\mathbf{G}_{k,1}, \mathbf{G}_{k,2}, \dots, \mathbf{G}_{k,P-1}$.

Let $\mathbf{d}_p(j)$, $p = 1, 2, \dots, P-1$ be the subvector of $\mathbf{d}(j)$ consisting of the elements of $\mathbf{d}(j)$ starting from $(p-1)L+1$ to $(p+1)L$. For unit-energy orthogonal spreading codes, the HR-DSCM receiver consists of the following steps:

- 1) Calculate the covariance matrices $\hat{\mathbf{R}}_{dx_k}$ and $\hat{\mathbf{R}}_{x_k x_k}$ as in (11) and (12), respectively.
- 2) Compute the estimates of \mathbf{A}_k , \mathbf{Q}_k and $\tilde{\mathbf{Q}}_k$, respectively, as in (13)–(15).
- 3) Let $\hat{\mathbf{A}}_{k,p}$, $p = 1, 2, \dots, P-1$ be the submatrix of $\hat{\mathbf{A}}_k$ consisting of the columns starting from $(p-1)L+1$ to $(p+1)L$, and determine the estimate $\tilde{\mathbf{A}}_{k,p}$ for each $\mathbf{d}_p(j)$, $p = 1, 2, \dots, P-1$:

$$\tilde{\mathbf{A}}_{k,p} = \hat{\mathbf{Q}}_k^{-1/2} \hat{\mathbf{A}}_{k,p} \triangleq \begin{bmatrix} \tilde{\mathbf{B}}_{k,p,0} & \tilde{\mathbf{B}}_{k,p,1} \end{bmatrix}. \quad (23)$$

- 4) Obtain the estimates of $\mathbf{G}_{k,p}$, $p = 1, 2, \dots, P-1$ as

$$\hat{\mathbf{G}}_{k,p} = \arg \max_{\mathbf{G}_{k,p} \in \mathcal{G}} \text{Re tr} \left\{ \mathbf{G}_{k,p} \tilde{\mathbf{B}}_{k,p,1}^H \tilde{\mathbf{Q}}_k \tilde{\mathbf{B}}_{k,p,0} \right\}. \quad (24)$$

Note that Steps 1 and 2 above are the same as those for DSCM, except that \mathbf{A}_k has a larger dimension. Steps 3 and 4 above are similar to those of DSCM and are repeated $P-1$ times.

The data rate of this HR-DSCM scheme is $P-1$ times that of the DSCM scheme presented in Section III. In general, the BER performance degrades as P increases. Yet a moderate value of P will only result in a slightly higher BER, as shown in Section V. However, a large value of P [such as for $P > 2J/(3L)$] will significantly degrade the performance of HR-DSCM. One reason for this to occur is the bias incurred in the \mathbf{Q}_k estimate (see Appendix B).

V. NUMERICAL EXAMPLES

We present numerical examples to demonstrate the performance of the proposed DSCM schemes. Five sets of examples are given in this section:

- 1) DSCM for time-invariant channels;
- 2) DSCM for time-varying channels;
- 3) HR-DSCM for time-invariant channels;
- 4) HR-DSCM for time-varying channels;
- 5) comparison between HR-DSCM and DSTM.

Unless otherwise stated, the DSCM, HR-DSCM, and DSTM schemes considered herein are all equipped with $M = 2$ transmit antennas and $N = 4$ ($N = 5$ in only one simulation example) receive antennas and employ the 2×2 unitary group code over the BPSK constellation, as described by (3). The space-time codes are constructed by using (7) for DSCM, (18)–(20) for HR-DSCM, and (2) for DSTM. For HR-DSCM and DSCM, $\mathbf{C}_{k,0}$ is chosen to be $\mathbf{C}_{k-1,P-1}$ and $\mathbf{C}_{k-1,1}$, respectively. Unit-energy Hadamard codes are used as spreading sequences in all simulations.

The interference and noise term $\mathbf{e}_k(j)$ in (8) is simulated as

$$\mathbf{e}_k(j) = \mathbf{n}_k(j) + \sum_{i=1}^I \sqrt{\rho_{k,i}} \mathbf{h}_{k,i} w_{k,i}(j) \quad (25)$$

where

$\mathbf{n}_k(j)$ additive zero-mean, unit variance, spatially, and temporally white complex Gaussian noise;

$w_{k,i}(j), i = 1, 2, \dots, I$ i th interference, which is temporally white complex Gaussian random process with zero-mean and unit variance;

$\mathbf{h}_{k,i}, i = 1, 2, \dots, I$ receiver array response to the interfering signal $w_{k,i}(j)$ with the elements of $\mathbf{h}_{k,i}$ modeled as i.i.d. zero-mean complex Gaussian random variables with unit variance;

$\rho_{k,i}, i = 1, 2, \dots, I$ power of the i th interference.

The interference-to-noise ratio (INR) for the i th interference signal is defined as $\rho_{k,i}, i = 1, 2, \dots, I$. The SNR $\tilde{\rho}$ per receive antenna for HR-DSCM is

$$\tilde{\rho} = PL\rho/J. \quad (26)$$

When time-varying fading is considered, \mathbf{H}_k and $\mathbf{h}_{k,i}, i = 1, 2, \dots, I$ are changed to $\mathbf{H}_k(j)$ and $\mathbf{h}_{k,i}(j), i = 1, 2, \dots, I$, respectively, which change from time sample to time sample, according to the Jakes' model [15].

As mentioned in Section III, J is a very important parameter for DSCM. Our simulation results show that $J = 32$ is a reasonable choice in that it is the smallest J that offers nearly the same BER as that of a larger J , such as $J = 64$. The results are consistent with the theoretical studies in [16] for adaptive arrays. In the following examples for DSCM and HR-DSCM, the spreading sequence length is fixed to $J = 32$.

A. DSCM for Time-Invariant Channels

Fig. 1 shows the BERs for DSCM as a function of the SNR for time-invariant fading channels when $I = 1$ and $J = 32$. Note that DSCM is very interference resistant.

The spreading sequences of DSCM can be used to mitigate the effects of interferences in a way similar to matched filters.

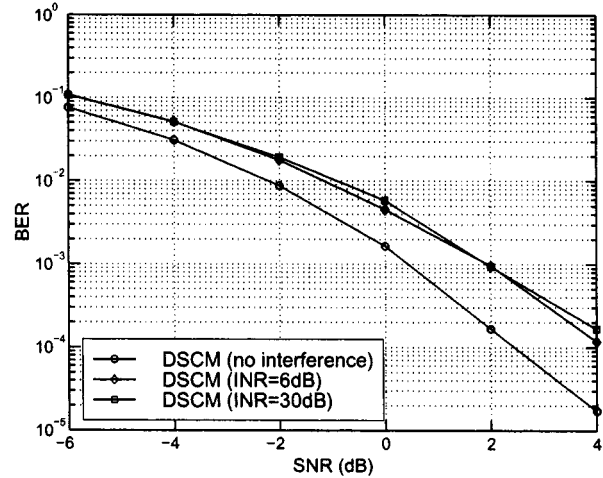


Fig. 1. BER versus SNR for DSCM for different INRs when the channel is time invariant.

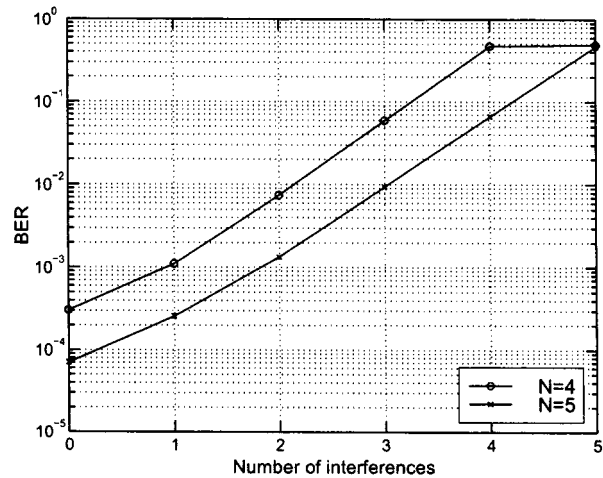


Fig. 2. BER versus I for DSCM for different numbers of receive antennas when the channel is time invariant, SNR = 2 dB, and INR = 30 dB.

However, using spreading sequences alone cannot achieve interference suppression. In effect, the interference suppression ability of DSCM is mainly due to the degree of freedom offered by the multiple receive antennas as a result of estimating the interference and noise covariance matrix \mathbf{Q}_k . Fig. 2 shows the BERs of DSCM as a function of I , which is the number of interfering signals, all of which have INR = 30 dB for SNR = 2 dB and for different numbers of antennas $N = 4$ and $N = 5$. As seen there, the number of interferences that can be effectively suppressed is $N - 1$, which are the spatial degrees of freedom.

B. DSCM for Time-Varying Channels

The channels in the following examples experience time-varying fading due to the relative motions of mobiles and/or surroundings. The time-varying fading is characterized by the normalized Doppler frequency $f_D T$, where f_D is the Doppler frequency, and $T = 1/B$ with B denoting the bandwidth.

Fig. 3 shows the BERs of DSCM as a function of the SNR for $f_D = 200$ Hz [corresponding to a vehicle moving at 75 mi/h with a carrier frequency 1.8 GHz] and $B = 512$ KHz.

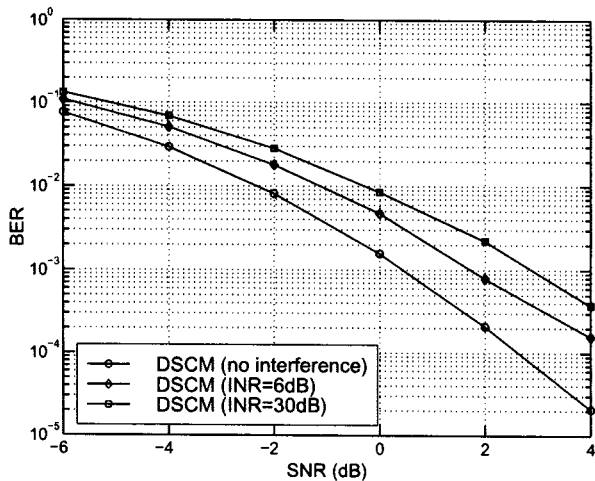


Fig. 3. BER versus SNR for DSCM for different INRs when the channel is time varying with $f_D = 200$ Hz and $B = 512$ KHz.

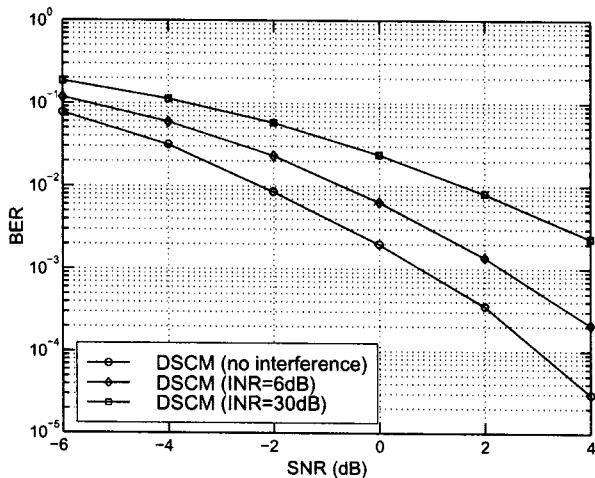


Fig. 4. BER versus SNR for DSCM for different INRs when the channel is time varying with $f_D = 200$ Hz and $B = 64$ KHz.

Fig. 4 shows the BERs when B is reduced to 64 KHz. Comparing Figs. 3 and 4 with Fig. 1, we observe that as expected, a larger bandwidth (higher data rate) makes DSCM more robust against time-varying fading channels than a narrower bandwidth (lower data rate).

Fig. 5 shows the BER performance of DSCM as a function of f_D for various INRs when $I = 1$, SNR = 2 dB, and $B = 64$ KHz. The maximum f_D is 400 Hz, which corresponds to a vehicle moving at 55 mi/h with a carrier frequency 5 GHz. Note that as f_D increases, the performance of DSCM degrades when strong interference exists. Additional simulations show that as expected, when $\mathbf{h}_{k,i}(j)$ varies with j , the number of interferences that can be effectively suppressed by DSCM decreases as a function of f_D . This is because the interferences no longer have fixed receiver array responses but time-varying ones. Hence, the receive antenna array can no longer form nulls at fixed $\mathbf{h}_{k,i}$, $i = 1, 2, \dots, I$. The situation can be improved by employing a larger receive antenna array.

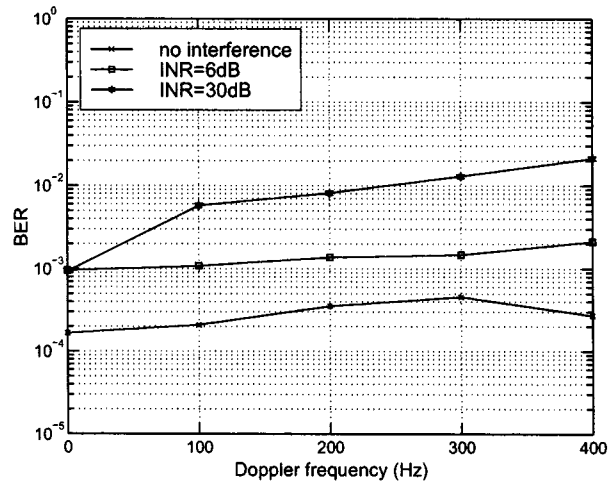


Fig. 5. BER versus Doppler frequency for DSCM for different INRs when the channel is time varying with $f_D = 200$ Hz, $B = 64$ KHz, and SNR = 2 dB.

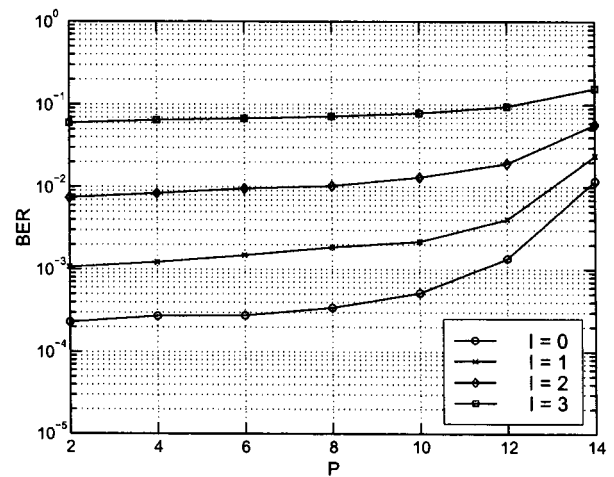


Fig. 6. BER versus P for HR-DSCM for different interference numbers when the channel is time invariant and INR = 30 dB.

C. HR-DSCM for Time-Invariant Channels

As shown in Appendix B, the estimate of \mathbf{Q}_k will be zero for unit-energy orthogonal sequences when $P = J/L$. Hence, the maximum P in the simulations is selected to be 14 for $J = 32$. The minimum P is 2, corresponding to the case of DSCM. Fig. 6 illustrates the BERs of HR-DSCM as a function of P for time-invariant fading channels for different numbers of interferences when each interference has INR = 30 dB. The transmitted power is chosen such that SNR = 2 dB for $P = 2$ (the DSCM case). Note that the SNR (defined as the ratio of the transmitted signal power to the noise power) for HR-DSCM is $PL\rho/J$. Fig. 6 shows that the performance of HR-DSCM degrades only slightly, even when P is as large as 10. This implies that we can still achieve interference suppression even when the data rate is increased significantly.

D. HR-DSCM for Time-Varying Channels

Fig. 7 is similar to Fig. 6, except that the channel is now time varying with $f_D = 200$ Hz and $B = 64$ KHz. We note that the

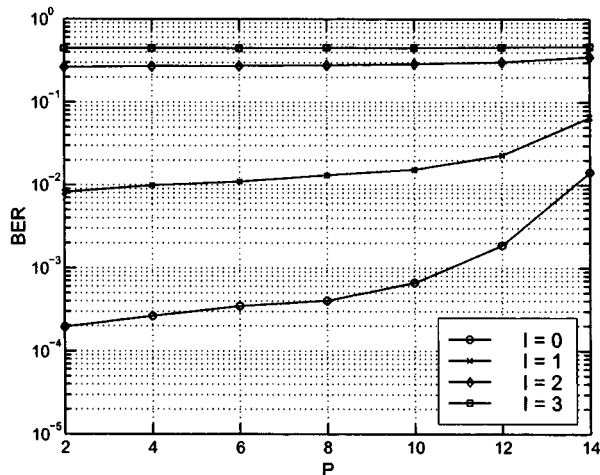


Fig. 7. BER versus P for HR-DSCM for different interference numbers when the channel is time varying with $f_D = 200$ Hz, $B = 64$ KHz, and INR = 30 dB.

performance of HR-DSCM degrades similarly to that of DSCM for time-varying channels.

E. Comparison Between HR-DSCM and DSTM

To show the performance of the HR-DSCM scheme in another perspective, we present comparison with the DSTM scheme employing error-correction coding, which is referred to as EC-DSTM. In the comparison, we use HR-DSCM with $P = 9$ and $J = 32$ to be compared with EC-DSTM for time-invariant channels. The comparison between HR-DSCM and EC-DSTM is based on the same bit rate (due to error-correction coding for EC-DSTM), SNR, and INR. (Note that EC-DSTM is a somewhat arbitrary approach to match the bit rates of the two schemes.) When the code shown in (3) is employed, the bit rate is 1/2 bits/s/Hz for HR-DSCM and 1 for DSTM. Therefore, to achieve the same net bit rate for EC-DSTM and HR-DSCM, the bit stream in the EC-DSTM system is encoded by using a convolutional code with rate 1/2 [17].

Fig. 8 shows the BERs of HR-DSCM and EC-DSTM as a function of the SNR for different INRs with $I = 1$ when the channel is time invariant. Note that in the presence of interference, HR-DSCM offers much better performance than EC-DSTM. (Note that the reason that EC-DSTM performs better than HR-DSCM at higher SNR in the absence of interference is due to the underlying error correcting code.)

VI. CONCLUSIONS

We have proposed a new spatial and temporal coding/modulation scheme, which is referred to as the *differential space-code modulation* (DSCM). We have shown that at the cost of a lower data rate or wider bandwidth or a combination of both, DSCM significantly outperforms DSTM when interferences, especially strong ones, are present. Moreover, the DSCM scheme requires less transmission power and hence is more suitable for covert communications. We have also extended the DSCM scheme to obtain a high-rate DSCM scheme that increases the data rate considerably at the cost of a slightly higher BER while still maintaining the interference suppression capability.

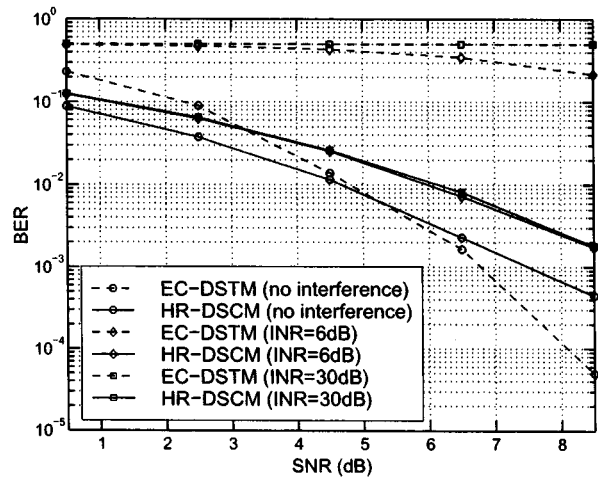


Fig. 8. BER versus SNR comparison between HR-DSCM and EC-DSTM for different INR's when $I = 1$.

APPENDIX A

DERIVATION OF THE DSCM RECEIVER

In this Appendix, we give a detailed derivation of our DSCM receiver for $M = L$. The DSCM receiver we derive below is not an exact maximum likelihood (ML) receiver since it appears difficult to obtain an exact ML receiver under the stochastic channel assumption.

Note that

$$\begin{aligned} \mathbf{R}_C &\triangleq \begin{bmatrix} \mathbf{C}_{k,0}^H & \\ \mathbf{C}_{k,1}^H & \end{bmatrix} [\mathbf{C}_{k,0} \quad \mathbf{C}_{k,1}] = \begin{bmatrix} \mathbf{F} & \mathbf{F}\mathbf{G}_k \\ \mathbf{G}_k^H \mathbf{F} & \mathbf{F} \end{bmatrix} \\ &= \begin{bmatrix} \mathbf{I} & \\ & \mathbf{G}_k^H \end{bmatrix} \mathbf{F} [\mathbf{I} \quad \mathbf{G}_k] \end{aligned} \quad (27)$$

where $\mathbf{F} \triangleq \mathbf{C}_{k,0}^H \mathbf{C}_{k,0} = \mathbf{C}_{k,1}^H \mathbf{C}_{k,1}$, which is due to the properties of the unitary group codes. When $M = L$, we have $\mathbf{F} = M\mathbf{I}$. Hence

$$\mathbf{R}_C = \begin{bmatrix} M\mathbf{I} & M\mathbf{G}_k \\ M\mathbf{G}_k^H & M\mathbf{I} \end{bmatrix}. \quad (28)$$

We also have

$$[\mathbf{C}_{k,0} \quad \mathbf{C}_{k,1}] \begin{bmatrix} \mathbf{C}_{k,0}^H \\ \mathbf{C}_{k,1}^H \end{bmatrix} = 2L\mathbf{I} \quad (29)$$

which is also due to the properties of the unitary group codes.

The log-likelihood function of

$$\begin{aligned} \mathbf{x}_k(j) &= \sqrt{\rho_M} \mathbf{H}_k [\mathbf{C}_{k,0} \quad \mathbf{C}_{k,1}] \mathbf{d}(j) + \mathbf{e}_k(j) \\ j &= 1, \dots, J \end{aligned} \quad (30)$$

is proportional to

$$-\ln |\mathbf{Q}_k| - \text{tr} \left\{ \mathbf{Q}_k^{-1} \frac{1}{J} \sum_{j=1}^J [\mathbf{x}_k(j) - \mathbf{A}_k \mathbf{d}(j)] \cdot [\mathbf{x}_k(j) - \mathbf{A}_k \mathbf{d}(j)]^H \right\}. \quad (31)$$

Then, the problem of estimating \mathbf{Q}_k and \mathbf{A}_k becomes similar to the one considered in [18].

Let

$$\hat{\mathbf{R}}_{dx_k} = \frac{1}{J} \sum_{j=1}^J \mathbf{d}(j) \mathbf{x}_k^H(j) \quad (32)$$

$$\hat{\mathbf{R}}_{dd} = \frac{1}{J} \sum_{j=1}^J \mathbf{d}(j) \mathbf{d}^H(j) \quad (33)$$

and

$$\hat{\mathbf{R}}_{x_k x_k} = \frac{1}{J} \sum_{j=1}^J \mathbf{x}_k(j) \mathbf{x}_k^H(j). \quad (34)$$

Equation (31) becomes

$$-\ln |\mathbf{Q}_k| - \text{tr} \left\{ \mathbf{Q}_k^{-1} \left[\hat{\mathbf{R}}_{x_k x_k} - \mathbf{A}_k \hat{\mathbf{R}}_{dx_k} - \hat{\mathbf{R}}_{dx_k}^H \mathbf{A}_k^H + \mathbf{A}_k \hat{\mathbf{R}}_{dd} \mathbf{A}_k^H \right] \right\}. \quad (35)$$

Then, the ML estimates of \mathbf{A}_k and \mathbf{Q}_k , respectively, are

$$\hat{\mathbf{A}}_k = \hat{\mathbf{R}}_{dx_k}^H \hat{\mathbf{R}}_{dd}^{-1} \quad (36)$$

and

$$\hat{\mathbf{Q}}_k = \hat{\mathbf{R}}_{x_k x_k} - \hat{\mathbf{R}}_{dx_k}^H \hat{\mathbf{R}}_{dd}^{-1} \hat{\mathbf{R}}_{dx_k}. \quad (37)$$

Note that

$$\begin{aligned} \hat{\mathbf{A}}_k &= \left[\frac{1}{J} \sum_{j=1}^J \mathbf{d}(j) \mathbf{x}_k^H(j) \right]^H \hat{\mathbf{R}}_{dd}^{-1} \\ &= \left\{ \frac{1}{J} \sum_{j=1}^J [\mathbf{A}_k \mathbf{d}(j) + \mathbf{e}_k(j)] \mathbf{d}^H(j) \right\} \hat{\mathbf{R}}_{dd}^{-1} \\ &= \mathbf{A}_k + \frac{1}{J} \left\{ \sum_{j=1}^J \mathbf{e}_k(j) \mathbf{d}^H(j) \right\} \hat{\mathbf{R}}_{dd}^{-1}. \end{aligned} \quad (38)$$

Let

$$\tilde{\mathbf{d}}(j) = \hat{\mathbf{R}}_{dd}^{-1} \mathbf{d}(j). \quad (39)$$

We have

$$\begin{aligned} \text{vec}(\hat{\mathbf{A}}_k) &= \text{vec}(\mathbf{A}_k) + \frac{1}{J} \sum_{j=1}^J \left(\tilde{\mathbf{d}}^*(j) \otimes \mathbf{I}_N \right) \mathbf{e}_k(j) \\ &\triangleq \text{vec}(\mathbf{A}_k) + \hat{\mathbf{e}}_k \end{aligned} \quad (40)$$

where we have used $\text{vec}(\mathbf{ABC}) = (\mathbf{C}^T \otimes \mathbf{A}) \text{vec}(\mathbf{B})$. For the $\hat{\mathbf{e}}_k$ in (40), we have

$$\begin{aligned} \text{E}[\hat{\mathbf{e}}_k \hat{\mathbf{e}}_k^H] &= \text{E} \left[\frac{1}{J^2} \sum_{j_1=1}^J \sum_{j_2=1}^J \left(\tilde{\mathbf{d}}^*(j_1) \otimes \mathbf{I}_N \right) \right. \\ &\quad \left. \cdot \mathbf{e}_k(j_1) \mathbf{e}_k^H(j_2) \left(\tilde{\mathbf{d}}^*(j_2) \otimes \mathbf{I}_N \right)^H \right] \end{aligned}$$

$$\begin{aligned} &= \frac{1}{J^2} \sum_{j=1}^J \left(\tilde{\mathbf{d}}^*(j) \otimes \mathbf{I}_N \right) \mathbf{Q}_k \left(\tilde{\mathbf{d}}^*(j) \otimes \mathbf{I}_N \right)^H \\ &= \frac{1}{J^2} \sum_{j=1}^J \left(\tilde{\mathbf{d}}^*(j) \tilde{\mathbf{d}}^T(j) \right) \otimes \mathbf{Q}_k \\ &= \frac{1}{J^2} \sum_{j=1}^J \left[\left(\hat{\mathbf{R}}_{dd}^{-1} \right)^* \mathbf{d}^*(j) \mathbf{d}^T(j) \left(\hat{\mathbf{R}}_{dd}^{-1} \right)^T \right] \otimes \mathbf{Q}_k \\ &= \frac{1}{J} \left(\hat{\mathbf{R}}_{dd}^{-1} \right)^T \otimes \mathbf{Q}_k. \end{aligned} \quad (41)$$

Consider the structure of

$$\mathbf{A}_k = \sqrt{\rho_M} \mathbf{H}_k [\mathbf{C}_{k,0} \quad \mathbf{C}_{k,1}]. \quad (42)$$

We have

$$\text{vec}(\mathbf{A}_k) = \sqrt{\rho_M} \left\{ \begin{bmatrix} \mathbf{C}_{k,0}^T \\ \mathbf{C}_{k,1}^T \end{bmatrix} \otimes \mathbf{I}_N \right\} \text{vec}(\mathbf{H}_k) \quad (43)$$

which means we have

$$\text{vec}(\hat{\mathbf{A}}_k) \sim \mathcal{N}(0, \Sigma) \quad (44)$$

where

$$\Sigma \triangleq \rho_M \mathbf{R}_C^* \otimes \mathbf{I}_N + \frac{1}{J} \left(\hat{\mathbf{R}}_{dd}^{-1} \right)^T \otimes \mathbf{Q}_k. \quad (45)$$

In the above derivation, we have used the fact that $\text{vec}(\mathbf{H}_k) \sim \mathcal{N}(0, \mathbf{I})$. At this step, we can use the following equation to estimate \mathbf{G}_k :

$$\begin{aligned} \hat{\mathbf{G}}_k &= \arg \max_{\mathbf{G}_k \in \mathcal{G}} \\ &\quad \left\{ -\ln |\Sigma| - \text{tr} \left[\Sigma^{-1} \text{vec}(\hat{\mathbf{A}}_k) \text{vec}^H(\hat{\mathbf{A}}_k) \right] \right\}. \end{aligned} \quad (46)$$

To estimate the transmission power, we also have

$$\text{tr}[\mathbf{A}_k \mathbf{A}_k^H] = \text{tr}[\rho_M \mathbf{H}_k (2M\mathbf{I}) \mathbf{H}_k^H]. \quad (47)$$

This means that

$$\text{E} \left\{ \text{tr}[\mathbf{A}_k \mathbf{A}_k^H] \right\} = 2M\rho_M(MN) = 2M^2N\rho_M. \quad (48)$$

Therefore, we have the estimate of ρ_M as

$$\hat{\rho}_M \simeq \frac{1}{2M^2N} \text{tr}[\mathbf{A}_k \mathbf{A}_k^H] \simeq \frac{1}{2M^2N} \text{tr}[\hat{\mathbf{A}}_k \hat{\mathbf{A}}_k^H]. \quad (49)$$

To speed up the computation, we need to exploit the special structure of the spreading sequences. For unit energy orthogonal sequences (such as the Hadamard code), we have

$$\hat{\mathbf{R}}_{dd} = \frac{1}{J} \sum_{j=1}^J \mathbf{d}(j) \mathbf{d}^H(j) = \frac{1}{J} \mathbf{I}. \quad (50)$$

Therefore, (36) and (37) will become, respectively

$$\hat{\mathbf{A}}_k = J \hat{\mathbf{R}}_{dx_k}^H \quad (51)$$

and

$$\hat{\mathbf{Q}}_k = \hat{\mathbf{R}}_{x_k x_k} - J \hat{\mathbf{R}}_{dx_k}^H \hat{\mathbf{R}}_{dx_k}. \quad (52)$$

Denote

$$\tilde{\mathbf{A}}_k = \hat{\mathbf{Q}}_k^{-1/2} \hat{\mathbf{A}}_k \quad (53)$$

and

$$\text{vec}(\tilde{\mathbf{A}}_k) = \left(\mathbf{I} \otimes \hat{\mathbf{Q}}_k^{-1/2} \right) \text{vec}(\mathbf{A}_k) + \tilde{\mathbf{e}}_k. \quad (54)$$

We have approximately

$$\tilde{\mathbf{e}}_k \sim \mathcal{N}(0, \mathbf{I}). \quad (55)$$

This is because

$$\begin{aligned} \mathbb{E}[\tilde{\mathbf{e}}_k \tilde{\mathbf{e}}_k^H] &= \mathbb{E} \left[\left(\mathbf{I} \otimes \hat{\mathbf{Q}}_k^{-1/2} \right) \mathbf{e}_k \mathbf{e}_k^H \left(\mathbf{I} \otimes \hat{\mathbf{Q}}_k^{-1/2} \right)^H \right] \\ &= \left(\mathbf{I} \otimes \hat{\mathbf{Q}}_k^{-1/2} \right) \left(\frac{1}{J} (J\mathbf{I}) \otimes \mathbf{Q}_k \right) \left(\mathbf{I} \otimes \hat{\mathbf{Q}}_k^{-1/2} \right)^H \\ &\simeq \mathbf{I}. \end{aligned} \quad (56)$$

From (43) and the fact that $\text{vec}(\mathbf{H}_k) \sim \mathcal{N}(0, \mathbf{I})$, we have

$$\text{vec}(\tilde{\mathbf{A}}_k) \sim \mathcal{N}(0, \tilde{\Sigma}) \quad (57)$$

where $\tilde{\Sigma} = \rho_M \Gamma + \mathbf{I}$, and

$$\begin{aligned} \Gamma &= \left(\mathbf{I} \otimes \hat{\mathbf{Q}}_k^{-1/2} \right) \left(\left[\begin{array}{c} \mathbf{C}_{k,0}^T \\ \mathbf{C}_{k,1}^T \end{array} \right] \otimes \mathbf{I}_N \right) \\ &\quad \cdot \left([\mathbf{C}_{k,0}^* \quad \mathbf{C}_{k,1}^*] \otimes \mathbf{I}_N \right) \left(\mathbf{I} \otimes \hat{\mathbf{Q}}_k^{-1/2} \right)^H \\ &= \left(\left[\begin{array}{c} \mathbf{C}_{k,0}^T \\ \mathbf{C}_{k,1}^T \end{array} \right] \otimes \hat{\mathbf{Q}}_k^{-1/2} \right) \left([\mathbf{C}_{k,0}^* \quad \mathbf{C}_{k,1}^*] \otimes \hat{\mathbf{Q}}_k^{-1/2} \right) \\ &\triangleq \Gamma_1 \Gamma_1^H. \end{aligned} \quad (58)$$

Now, we calculate the determinant and inversion of $\tilde{\Sigma}$. First

$$\begin{aligned} |\tilde{\Sigma}| &= |\mathbf{I} + \rho_M \Gamma_1 \Gamma_1^H| \\ &= |\mathbf{I} + \rho_M \Gamma_1^H \Gamma_1| \\ &= \left| \mathbf{I} + \rho_M \left([\mathbf{C}_{k,0}^* \quad \mathbf{C}_{k,1}^*] \begin{bmatrix} \mathbf{C}_{k,0}^T \\ \mathbf{C}_{k,1}^T \end{bmatrix} \right) \otimes \hat{\mathbf{Q}}_k^{-1} \right| \\ &= \left| \mathbf{I} + 2M\rho_M \left(\mathbf{I} \otimes \hat{\mathbf{Q}}_k^{-1} \right) \right| \end{aligned} \quad (59)$$

which means that $|\tilde{\Sigma}|$ is independent of \mathbf{G}_k ! In the above derivation, we have used the fact that $|\mathbf{I} + \mathbf{A}\mathbf{B}| = |\mathbf{I} + \mathbf{B}\mathbf{A}|$ whenever the dimensions of \mathbf{A} and \mathbf{B} are conformable. Then

$$\begin{aligned} \tilde{\Sigma}^{-1} &= \left(\mathbf{I} + \rho_M \Gamma_1 \Gamma_1^H \right)^{-1} \\ &= \mathbf{I} + \Gamma_1 \left(-\frac{1}{\rho_M} \mathbf{I} - \Gamma_1^H \Gamma_1 \right)^{-1} \Gamma_1^H \\ &= \mathbf{I} + \left(\left[\begin{array}{c} \mathbf{C}_{k,0}^T \\ \mathbf{C}_{k,1}^T \end{array} \right] \otimes \hat{\mathbf{Q}}_k^{-1/2} \right) \\ &\quad \cdot \left(-\frac{1}{\rho_M} \mathbf{I} - 2M \left(\mathbf{I} \otimes \hat{\mathbf{Q}}_k^{-1} \right) \right)^{-1} \end{aligned}$$

$$\begin{aligned} &\cdot \left([\mathbf{C}_{k,0}^* \quad \mathbf{C}_{k,1}^*] \otimes \hat{\mathbf{Q}}_k^{-1/2} \right) \\ &= \mathbf{I} + \left(\left[\begin{array}{c} \mathbf{C}_{k,0}^T \\ \mathbf{C}_{k,1}^T \end{array} \right] \otimes \hat{\mathbf{Q}}_k^{-1/2} \right) \\ &\quad \cdot \left(\mathbf{I} \otimes \left[-\frac{1}{\rho_M} \mathbf{I} - 2M\hat{\mathbf{Q}}_k^{-1} \right] \right)^{-1} \\ &\quad \cdot \left([\mathbf{C}_{k,0}^* \quad \mathbf{C}_{k,1}^*] \otimes \hat{\mathbf{Q}}_k^{-1/2} \right) \\ &= \mathbf{I} - \rho_M \mathbf{R}_C^* \otimes \left(\hat{\mathbf{Q}}_k^{-1/2} \left(\mathbf{I} + 2M\rho_M \hat{\mathbf{Q}}_k^{-1} \right)^{-1} \hat{\mathbf{Q}}_k^{-1/2} \right) \\ &= \mathbf{I} - \rho_M \mathbf{R}_C^* \otimes \tilde{\mathbf{Q}}_k \end{aligned} \quad (60)$$

where

$$\tilde{\mathbf{Q}}_k \triangleq \hat{\mathbf{Q}}_k^{-1/2} \left(\mathbf{I} + 2M\rho_M \hat{\mathbf{Q}}_k^{-1} \right)^{-1} \hat{\mathbf{Q}}_k^{-1/2}. \quad (61)$$

Replacing the above ρ_M with the $\hat{\rho}_M$ in (49) yields

$$\hat{\mathbf{G}}_k = \arg \max_{\mathbf{G}_k \in \mathcal{G}} \text{tr} \left[\left(\mathbf{R}_C^* \otimes \tilde{\mathbf{Q}}_k \right) \text{vec}(\tilde{\mathbf{A}}_k) \text{vec}^H(\tilde{\mathbf{A}}_k) \right]. \quad (62)$$

Dividing $\tilde{\mathbf{A}}_k$ into two $N \times L$ submatrices, i.e., $\tilde{\mathbf{A}}_k = [\tilde{\mathbf{B}}_{k,0} \quad \tilde{\mathbf{B}}_{k,1}]$, we have

$$\text{vec}(\tilde{\mathbf{A}}_k) = \text{vec} \left([\tilde{\mathbf{B}}_{k,0} \quad \tilde{\mathbf{B}}_{k,1}] \right). \quad (63)$$

Hence

$$\left(\mathbf{R}_C^* \otimes \tilde{\mathbf{Q}}_k \right) \text{vec}(\tilde{\mathbf{A}}_k) = \text{vec} \left(\tilde{\mathbf{Q}}_k \left[\tilde{\mathbf{B}}_{k,0} \quad \tilde{\mathbf{B}}_{k,1} \right] \mathbf{R}_C \right) \quad (64)$$

and

$$\begin{aligned} f(\mathbf{G}_k) &\triangleq \text{tr} \left[\left(\mathbf{R}_C^* \otimes \tilde{\mathbf{Q}}_k \right) \text{vec}(\tilde{\mathbf{A}}_k) \text{vec}^H(\tilde{\mathbf{A}}_k) \right] \\ &= \text{vec}^H(\tilde{\mathbf{A}}_k) \text{vec} \left(\tilde{\mathbf{Q}}_k \left[\tilde{\mathbf{B}}_{k,0} \quad \tilde{\mathbf{B}}_{k,1} \right] \mathbf{R}_C \right) \\ &= \text{tr} \left\{ \tilde{\mathbf{Q}}_k \left[\tilde{\mathbf{B}}_{k,0} \quad \tilde{\mathbf{B}}_{k,1} \right] \begin{bmatrix} M\mathbf{I} & M\mathbf{G}_k \\ M\mathbf{G}_k^H & M\mathbf{I} \end{bmatrix} \right. \\ &\quad \left. \cdot \begin{bmatrix} \tilde{\mathbf{B}}_{k,0}^H \\ \tilde{\mathbf{B}}_{k,1}^H \end{bmatrix} \right\} \\ &= M \text{tr} \left\{ \tilde{\mathbf{Q}}_k \tilde{\mathbf{B}}_{k,0} \tilde{\mathbf{B}}_{k,0}^H + \tilde{\mathbf{Q}}_k \tilde{\mathbf{B}}_{k,1} \mathbf{G}_k^H \tilde{\mathbf{B}}_{k,0}^H \right. \\ &\quad \left. + \tilde{\mathbf{Q}}_k \tilde{\mathbf{B}}_{k,0} \mathbf{G}_k \tilde{\mathbf{B}}_{k,1}^H + \tilde{\mathbf{Q}}_k \tilde{\mathbf{B}}_{k,1} \tilde{\mathbf{B}}_{k,1}^H \right\}. \end{aligned} \quad (65)$$

We only need to consider the terms involving \mathbf{G}_k , i.e.,

$$\begin{aligned} &\text{tr} \left\{ \tilde{\mathbf{Q}}_k \tilde{\mathbf{B}}_{k,1} \mathbf{G}_k^H \tilde{\mathbf{B}}_{k,0}^H + \tilde{\mathbf{Q}}_k \tilde{\mathbf{B}}_{k,0} \mathbf{G}_k \tilde{\mathbf{B}}_{k,1}^H \right\} \\ &= 2\text{Re} \text{tr} \left\{ \tilde{\mathbf{Q}}_k \tilde{\mathbf{B}}_{k,0} \mathbf{G}_k \tilde{\mathbf{B}}_{k,1}^H \right\} \\ &= 2\text{Re} \text{tr} \left\{ \mathbf{G}_k \tilde{\mathbf{B}}_{k,1}^H \tilde{\mathbf{Q}}_k \tilde{\mathbf{B}}_{k,0} \right\}. \end{aligned} \quad (66)$$

As a result, we have

$$\hat{\mathbf{G}}_k = \arg \max_{\mathbf{G}_k \in \mathcal{G}} \text{Re} \text{tr} \left\{ \mathbf{G}_k \tilde{\mathbf{B}}_{k,1}^H \tilde{\mathbf{Q}}_k \tilde{\mathbf{B}}_{k,0} \right\}. \quad (67)$$

APPENDIX B
PROPERTIES OF $\hat{\mathbf{Q}}_k$

In this Appendix, we examine the properties of $\hat{\mathbf{Q}}_k$. We consider the high-rate DSCM scheme and unit energy orthogonal spreading sequences. Note that

$$\mathbf{A}_k = \sqrt{\rho_M} \mathbf{H}_k [\mathbf{C}_{k,0} \quad \mathbf{C}_{k,1} \quad \cdots \quad \mathbf{C}_{k,(P-1)}]. \quad (68)$$

From the definition, we have

$$\begin{aligned} \hat{\mathbf{R}}_{x_k x_k} &= \frac{1}{J} \sum_{j=1}^J \mathbf{x}_k(j) \mathbf{x}_k^H(j) \\ &= \frac{1}{J} \sum_{j=1}^J [\mathbf{A}_k \mathbf{d}(j) + \mathbf{e}_k(j)] [\mathbf{A}_k \mathbf{d}(j) + \mathbf{e}_k(j)]^H \\ &= \frac{1}{J} \sum_{j=1}^J \{ \mathbf{A}_k \mathbf{d}(j) \mathbf{d}^H(j) \mathbf{A}_k^H + \mathbf{e}_k(j) \mathbf{e}_k^H(j) \\ &\quad + 2\text{Re} [\mathbf{A}_k \mathbf{d}(j) \mathbf{e}_k^H(j)] \} \\ &= \frac{1}{J} \mathbf{A}_k \mathbf{A}_k^H + \frac{1}{J} \sum_{j=1}^J \mathbf{e}_k(j) \mathbf{e}_k^H(j) \\ &\quad + 2\text{Re} \left[\mathbf{A}_k \frac{1}{J} \sum_{j=1}^J \mathbf{d}(j) \mathbf{e}_k^H(j) \right] \end{aligned} \quad (69)$$

and

$$\begin{aligned} \hat{\mathbf{R}}_{dx_k} &= \frac{1}{J} \sum_{j=1}^J \mathbf{d}(j) \mathbf{x}_k^H(j) \\ &= \frac{1}{J} \sum_{j=1}^J \mathbf{d}(j) [\mathbf{A}_k \mathbf{d}(j) + \mathbf{e}_k(j)]^H \\ &= \frac{1}{J} \mathbf{A}_k^H + \frac{1}{J} \sum_{j=1}^J \mathbf{d}(j) \mathbf{e}_k^H(j). \end{aligned} \quad (70)$$

Using (70), we have

$$\begin{aligned} \hat{\mathbf{R}}_{dx_k}^H \hat{\mathbf{R}}_{dx_k} &= \frac{1}{J^2} \mathbf{A}_k \mathbf{A}_k^H \\ &\quad + \frac{1}{J^2} \sum_{j_1=1}^J \sum_{j_2=1}^J \mathbf{e}_k(j_1) \mathbf{d}^H(j_1) \mathbf{d}(j_2) \mathbf{e}_k^H(j_2) \\ &\quad + 2\text{Re} \left[\mathbf{A}_k \frac{1}{J^2} \sum_{j=1}^J \mathbf{d}(j) \mathbf{e}_k^H(j) \right]. \end{aligned} \quad (71)$$

Hence

$$\begin{aligned} \hat{\mathbf{Q}}_k &= \hat{\mathbf{R}}_{x_k x_k} - J \hat{\mathbf{R}}_{dx_k}^H \hat{\mathbf{R}}_{dx_k} \\ &= \frac{1}{J} \sum_{j=1}^J \mathbf{e}_k(j) \mathbf{e}_k^H(j) \\ &\quad - \frac{1}{J} \sum_{j_1=1}^J \sum_{j_2=1}^J \mathbf{e}_k(j_1) \mathbf{d}^H(j_1) \mathbf{d}(j_2) \mathbf{e}_k^H(j_2) \end{aligned}$$

$$\begin{aligned} &= \frac{1}{J} \sum_{j=1}^J \mathbf{e}_k(j) \mathbf{e}_k^H(j) - \frac{1}{J} \sum_{j=1}^J \mathbf{e}_k(j) \mathbf{d}^H(j) \mathbf{d}(j) \mathbf{e}_k^H(j) \\ &\quad - \frac{1}{J} \sum_{j_1=1, j_2=1, j_1 \neq j_2}^J \mathbf{e}_k(j_1) \mathbf{d}^H(j_1) \mathbf{d}(j_2) \mathbf{e}_k^H(j_2) \\ &= \frac{J-PL}{J^2} \sum_{j=1}^J \mathbf{e}_k(j) \mathbf{e}_k^H(j) \\ &\quad - \frac{1}{J} \sum_{j_1=1, j_2=1, j_1 \neq j_2}^J \mathbf{e}_k(j_1) \mathbf{d}^H(j_1) \mathbf{d}(j_2) \mathbf{e}_k^H(j_2) \end{aligned} \quad (72)$$

where we have used the fact that $\mathbf{d}^H(j) \mathbf{d}(j) = PL/J$, $j = 1, 2, \dots, J$, which is determined by the definition of $\mathbf{d}(j)$, $j = 1, 2, \dots, J$. Hence

$$\mathbb{E} [\hat{\mathbf{Q}}_k] = \frac{J-PL}{J} \mathbf{Q}_k. \quad (73)$$

This means that when the number of columns of \mathbf{A}_k is large, $\hat{\mathbf{Q}}_k$ will be seriously biased. In the extreme case of $P = J/L$, $\hat{\mathbf{Q}}_k = 0$. This is due to the fact that $\mathbf{d}^H(j_1) \mathbf{d}(j_2) = 0$, $\forall j_1 \neq j_2$ when $P = J/L$.

REFERENCES

- [1] G. J. Foschini, Jr. and M. J. Gans, "On the limits of wireless communications in a fading environment when using multiple antennas," *Wireless Pers. Commun.*, Mar. 1998.
- [2] I. E. Telatar, "Capacity of multiple antenna Gaussian channels," *AT&T Tech. Memo.*, June 1995.
- [3] A. F. Naguib, N. Seshadri, and A. R. Calderbank, "Increasing data rate over wireless channels," *IEEE Signal Processing Mag.*, vol. 17, pp. 76–92, May 2000.
- [4] S. M. Alamouti, "A simple transmit diversity techniques for wireless communications," *IEEE J. Select. Areas Commun.*, vol. 16, pp. 1451–1458, Oct. 1998.
- [5] J. C. Guey, M. P. Fitz, M. R. Bell, and W. Y. Kuo, "Signal design for transmitter diversity wireless communication systems over rayleigh fading channels," in *Proc. IEEE Veh. Technol. Conf.*, 1996, pp. 136–140.
- [6] N. Seshadri and J. J. Winters, "Two signaling schemes for improving the error performance of frequency-division-duplex (FDD) transmission systems using transmitter antenna diversity," *Int. J. Wireless Inform. Networks*, vol. 1, no. 1, 1994.
- [7] A. Wittneben, "A new bandwidth efficient transmit antenna modulation diversity scheme for linear digital modulation," in *Proc. IEEE Integrated Circuits Conf.*, 1993, pp. 1630–1634.
- [8] B. L. Hughes, "Differential space-time modulation," in *Proc. 1999 IEEE Wireless Commun. Networking Conf.*, New Orleans, LA, Sept. 22–29, 1999.
- [9] B. M. Hochwald and W. Sweldens, "Differential unitary space-time modulation," *IEEE Trans. Commun.*, vol. 48, pp. 2041–2052, Dec. 2000.
- [10] V. Tarokh and H. Jafarkhani, "A differential detection scheme for transmit diversity," *IEEE J. Select. Areas Commun.*, vol. 18, pp. 1169–1174, July 2000.
- [11] B. L. Hughes, "Differential space-time modulation," *IEEE Trans. Inform. Theory*, vol. 46, pp. 2567–2578, Nov. 2000.
- [12] —, "Optimal space-time constellations from groups," *IEEE Trans. Inform. Theory*, 2000, submitted for publication.
- [13] B. M. Hochwald and T. L. Marzetta, "Unitary space-time modulation for multiple-antenna communications in Rayleigh flat fading," *IEEE Trans. Inform. Theory*, vol. 46, pp. 543–564, Mar. 2000.
- [14] B. M. Hochwald, T. L. Marzetta, T. Richardson, W. Sweldens, and R. Urbanke, "Systematic design of unitary space-time constellations," *IEEE Trans. Inform. Theory*, vol. 46, pp. 1962–1973, Sept. 2000.
- [15] W. C. Jakes, Jr., *Microwave Mobile Communications*. Piscataway, NJ: IEEE, 1993.

- [16] I. S. Reed, J. D. Mallett, and L. E. Brennan, "Rapid convergence rate in adaptive arrays," *IEEE Trans. Aerosp. Electron. Syst.*, vol. AES-10, pp. 853–863, Nov. 1974.
- [17] J. G. Proakis, *Digital Communications*, third ed: McGraw-Hill, 1995.
- [18] J. Li, B. Halder, P. Stoica, and M. Viberg, "Computationally efficient angle estimation for signals with known waveforms," *IEEE Trans. Signal Processing*, vol. 43, pp. 2154–2163, Sept. 1995.



Jianhua Liu (S'01) received the B.S. degree from Dalian Maritime University, Dalian, China, in 1984, the M.S. degree from the University of Electronic Science and Technology of China, Chengdu, in 1987, and the Ph.D. degree from Tsinghua University, Beijing, China, in 1998, all in electrical engineering. Since June 2000, he has been a Research Assistant with the Department of Electrical and Computer Engineering, University of Florida, Gainesville, pursuing the Ph.D. degree majoring in electrical engineering and minoring in statistics.

From February 1987 to February 1999, he worked at the Communications, Telemetry, and Telecontrol Research Institute, Shijiazhuang, China, where he was an Assistant Engineer, Engineer, Senior Engineer, and Research Fellow. From March 1995 to August 1998, he was also a Research Assistant at Tsinghua University. From February 1999 to June 2000, he worked at Nanyang Technological University, Singapore, as a Research Fellow. His research interests include wireless communications, statistical signal processing, and sensor array processing.



Jian Li (S'87–M'91–SM'97) received the M.Sc. and Ph.D. degrees in electrical engineering from The Ohio State University (OSU), Columbus, in 1987 and 1991, respectively.

From April 1991 to June 1991, she was an Adjunct Assistant Professor with the Department of Electrical Engineering, OSU. From July 1991 to June 1993, she was an Assistant Professor with the Department of Electrical Engineering, University of Kentucky, Lexington. Since August 1993, she has been with the Department of Electrical and Computer Engineering,

University of Florida, Gainesville, where she is currently a Professor. Her current research interests include spectral estimation, array signal processing, and signal processing for wireless communications and radar. She is a Guest Editor for *Multidimensional Systems and Signal Processing*.

Dr. Li is a member of Sigma Xi and Phi Kappa Phi. She received the 1994 National Science Foundation Young Investigator Award and the 1996 Office of Naval Research Young Investigator Award. She is currently an Associate Editor for *IEEE TRANSACTIONS ON SIGNAL PROCESSING*.



Hongbin Li (S'98–M'99) received the B.S. and M.S. degrees from the University of Electronic Science and Technology of China, Chengdu, in 1991 and 1994, respectively, and the Ph.D. degree from the University of Florida, Gainesville, in 1999, all in electrical engineering.

From July 1996 to May 1999, he was a Research Assistant with the Department of Electrical and Computer Engineering, University of Florida. Since July 1999, he has been an Assistant Professor with the Department of Electrical and Computer Engineering,

Stevens Institute of Technology, Hoboken, NJ. His current research interests include wireless communications, statistical signal processing, sensor array processing, and radar imaging.

Dr. Li is a member of Tau Beta Pi and Phi Kappa Phi. He received the 1999 Sigma Xi Graduate Research Award.



Erik G. Larsson (S'99) received the M.Sc. degree in applied physics and electrical engineering from Linköping University, Linköping, Sweden, in 1997. He is currently pursuing the Ph.D. degree with the Department of Systems and Control, Uppsala University, Uppsala, Sweden.

From 1998 to 1999, he was a Research Engineer with Ericsson Radio Systems AB, Stockholm, Sweden, where he was involved in the algorithm design and standardization of location services for the GSM System. He is currently on leave from

Uppsala University and is visiting the Department of Electrical and Computer Engineering, University of Florida, Gainesville. His research interests include statistical signal processing, wireless communications, spectral analysis, and radar applications.